A Distributionally Robust Chance-Constrained MILP Model for Multistage Distribution System Planning with Uncertain Renewables and Loads

Alireza Zare, *Student Member, IEEE*, C. Y. Chung, *Fellow, IEEE*, Junpeng Zhan, *Member, IEEE*, and Sherif Omar Faried, *Senior Member, IEEE*

***Abstract*—Successful transition to active distribution networks (ADNs) requires a planning methodology that includes an accurate network model and accounts for the major sources of uncertainty. Considering these two essential features, this paper proposes a novel model for the multistage distribution expansion planning (MDEP) problem, which is able to jointly expand both the network assets (feeders and substations) and renewable/conventional distributed generators (DGs). With respect to network characteristics, the proposed planning model employs a convex conic quadratic format of AC power flow equations that is linearized using a highly accurate polyhedral-based linearization method. Furthermore, a chance-constrained programming (CCP) approach is utilized to deal with the uncertain renewables and loads. In this regard, as the probability distribution functions (PDFs) of uncertain parameters are not perfectly known, a distributionally robust (DR) reformulation is proposed for the chance constraints (CCs) that guarantees the robustness of the expansion plans against all uncertainty distributions defined within a moment-based ambiguity set. Effective linearization techniques are also devised to eliminate the nonlinearities of the proposed DR reformulation, which yields a distributionally robust chance-constrained mixed-integer linear programming (DRCC-MILP) model for the MDEP problem of ADNs. Finally, the 24-node and 138-node test systems are used to demonstrate the effectiveness of the proposed planning methodology.**

***Index Terms*— Chance-constrained programming, distributionally robust optimization, mixed-integer linear programming (MILP), multistage distribution expansion planning (MDEP).**

I. NOMENCLATURE

A. Sets/Indices

$\Omega^a / a\ ,\ \omega$	Set/indices of conductor types.
$\Omega^b / \ b$	Set/index of alternatives for substations.
$\Omega^F / \ ij\ ,\ ki$	Set/indices of feeder sections ($\Omega^{FC} \cup \Omega^{FI} \cup \Omega^{FR}$).
Ω^{FC}	Set of candidate feeder sections for construction.
Ω^{FI}	Set of existing irreplaceable feeder sections.
Ω^{FR}	Set of existing replaceable feeder sections.
$\Omega^{gc} / \ g$	Set/index of alternatives for conventional DGs.
$\Omega^{gr} / \ g$	Set/index of alternatives for renewable DGs.
$\Omega^N / \ i\ ,\ j$	Set/indices of nodes ($\Omega^{NG} \cup \Omega_t^{NL} \cup \Omega^{NS} \cup \Omega_t^{NT}$).
Ω^{NG}	Set of candidate nodes for DG installation.
$\Omega_t^{NL}, \Omega^{NS}$	Sets of load and substation nodes, respectively.
Ω_t^{NT}	Set of transfer nodes.
Ω^S	Set of substations ($\Omega^{SC} \cup \Omega^{SR}$).
Ω^{SC}	Set of candidate substations for construction.
Ω^{SR}	Set of existing reinforceable substations.
$\Omega^T / \ t, v$	Set/indices of planning stages.

C. Constants

a_{ij}^{FI}, a_{ij}^{FR}	Initial conductor types of existing irreplaceable and replaceable feeder sections, respectively.
c^E	Energy cost ($/MWh).
c_g^{EGC}	Generation cost of conventional DGs ($/MWh).
c_a^{FC}, c_a^{FR}	Investment costs required to construct and replace feeder sections, respectively ($/km).
c_g^{GC}, c_g^{GR}	Investment costs required to install conventional and renewable DGs, respectively ($).
c_b^{SC}, c_b^{SR}	Investment costs required to construct and reinforce substations, respectively ($).
c_i^{SO}	Operation cost of substations ($/MWh).
D	Number of years in each planning stage.
$\overline{I_a}$	Maximum current flow of conductors (kA).
l_{ij}	Length of feeder sections (km).
$\overline{N^{GC}}, \overline{N^{GR}}$	Maximum number of installed DGs.
$\overline{\overline{P_{i,t}^D}}, \overline{\overline{Q_{i,t}^D}}$	Expected active and reactive power demands of load nodes, respectively (MW, MVAR).
$\overline{P_g^{GC}}, \overline{Q_g^{GC}}$	Upper limits for active and reactive powers of conventional DGs, respectively (MW, MVAR).
$\overline{\overline{P_g^{GR}}}$	Expected active power of renewable DGs (MW).
r	Annual interest rate.
R_a, X_a, Z_a	Resistance, reactance, and impedance of conductors, respectively (Ω/km).
$\overline{S_b}$	Capacity of alternatives for substations (MVA).
S_i^0	Initial capacity of existing substations (MVA).
$\underline{V}, \overline{V}$	Lower and upper voltage magnitude limits (kV).
$\overline{\Delta V}$	Upper bound of the variable $\Delta V_{ij,t}$.
$\tilde{\theta}_{i,t}^D$	Fictitious current flow demand of load nodes.
ρ^{GR}	Power factor of renewable DGs.
τ	Number of hours in one year.
ϕ^S	Loss factor of substations.

D. Decision Variables

$f_{ij,a,t}^F$	Square of current flow of feeder sections.
$f_{i,t}^S$	Square of current flow provided by substations.
$P_{ij,a,t}^F, Q_{ij,a,t}^F$	Active and reactive power flows of feeder sections, respectively (MW, MVAR).
$P_{i,g,t}^{GC}, Q_{i,g,t}^{GC}$ $P_{i,g,t}^{GR}, Q_{i,g,t}^{GR}$	Active and reactive powers of conventional and renewable DGs, respectively (MW, MVAR).
$P_{i,t}^S\ ,\ Q_{i,t}^S$	Active and reactive powers provided by substations, respectively (MW, MVAR).
$S_{ij,a,t}^F$	Apparent power flow of feeder sections (MVA).
$S_{i,t}^S$	Apparent power provided by substations (MVA).
$u_{i,t}$	Square of voltage magnitude of nodes.
$x_{ij,a,t}^{FC}, x_{ij,a,t}^{FR}$	Binary investment variables for construction and replacement of feeder sections, respectively.
$x_{i,g,t}^{GC}, x_{i,g,t}^{GR}$	Binary investment variables for installation of conventional and renewable DGs, respectively.
$x_{i,b,t}^{SC}, x_{i,b,t}^{SR}$	Binary investment variables for construction and reinforcement of substations, respectively.
$y_{ij,a,t}\ ,\ z_{i,t}$	Binary utilization variables of feeder sections and transfer nodes, respectively.

The work was supported in part by the Natural Sciences and Engineering Research Council (NSERC) of Canada and the Saskatchewan Power Corporation (SaskPower).

Alireza Zare, C. Y. Chung, Junpeng Zhan, and Sherif Omar Faried are with the Department of Electrical and Computer Engineering, University of Saskatchewan, Saskatoon, SK S7N 5A9, Canada (e-mail: alireza.zare@usask.ca, c.y.chung@usask.ca, j.p.zhan@usask.ca, sherif.faried@usask.ca).

$\Delta V_{ij,t}$ Auxiliary variable used for applying Kirchhoff's voltage law to feeder sections.

$\tilde{\theta}_{ij,t}^{F}$ Fictitious current flow of feeder sections.

$\tilde{\theta}_{i,t}^{S}$ Fictitious current supplied by substations.

II. Introduction

Over the last few years, driven by several technical and environmental factors, there has been a growing interest in the concept of active distribution networks (ADNs) [1]. Based on this new concept, traditional passive distribution networks will evolve into modern active ones by employing distributed energy resources (DERs) such as distributed generators (DGs) and demand responsive loads (DRLs) [2]. This transition from passive to active networks poses serious challenges to distribution system planners. On the one hand, the ability of DGs to directly inject active and reactive powers into the system nodes leads to bidirectional power flows through the distribution feeders [2]. This issue, if not adequately addressed at the design stage, can adversely affect various operational aspects of ADNs, such as reactive power balance and voltage regulation. Thus, the new context in which DGs come into play necessitates the development of a planning methodology that incorporates an accurate network model reflecting realistic operational characteristics of the system. On the other hand, large-scale integration of renewable DGs results in intermittent and volatile nodal power injections [3], [4], and the implementation of demand response programs further complicates the long-term predictability of load growth [2]. These factors introduce a huge amount of uncertainty to the planning process of ADNs. Hence, effective approaches must also be devised to properly model the major sources of uncertainty.

Based on the above discussion, obtaining economic, reliable, and robust expansion plans for ADNs requires a planning methodology that has two key features:

Feature 1: It should consider an accurate network model representing AC power flow equations and energy losses.

Feature 2: It should adequately account for the uncertainties associated with renewable DGs and loads.

This paper aims to develop a multistage distribution expansion planning (MDEP) model that is able to jointly expand both the network assets (feeders and substations) and DG units over the course of a number of planning stages, while giving full consideration to the above-mentioned key features.

Recently, many researchers have devoted their attention to modelling the MDEP problem in the context of ADNs [5]. The following presents a careful review of the current literature from the perspective of the noted features.

From the perspective of Feature 1, the existing MDEP models can be categorized into two groups: nonlinear and linear. The first group of MDEP models precisely reflect the nonlinear characteristics of the network (i.e., AC power flow equations and energy losses), but they are formulated as mixed-integer nonlinear programming (MINLP) problems that are very difficult to solve [1], [6-9]. For instance, the authors of [7] propose an optimization model for the MDEP problem in the presence of DGs, which aims to enhance the reliability levels of distribution networks. This model has a nonlinear formulation involving many local optimums and is solved using a modified version of the particle swarm optimization (PSO) algorithm. In [9], a Pareto-based multi-objective problem formulation subject to AC power flow constraints is proposed to determine the optimal size and location of DGs, where a hybrid evolutionary approach based on the combination of the PSO and shuffled frog-leaping (SFL) algorithms is employed to solve the problem. As can be seen, the MINLP models are solved using heuristic methods that not only cannot guarantee obtaining the global optimal solution, but also require a large computational effort. Moreover, these methods do not provide a measure of the quality of the obtained solution as they cannot estimate the distance to the global optimum.

To overcome the above drawbacks, the second group of MDEP models are presented in the form of mixed-integer linear programming (MILP) problems achieved by eliminating the nonlinearities of the network model [3], [4], [10-16], but these models have their own shortcomings. For instance, an MILP model, based on an extension of the linear disjunctive model normally used in the expansion planning of transmission networks, is proposed for the MDEP problem in [10]. This linear model is obtained by making some simplifications, such as employing DC power flow equations and ignoring energy losses. Similarly, the authors of [3], [4] propose an MILP model incorporating an adapted version of DC power flow equations, where energy loss and reactive power balance (i.e., the essential factors in any study on ADNs) are entirely neglected. Using these simplified network models may cause the solutions found for the MDEP problem to be optimistic or even deficient. The MILP models presented in [11-13] have a relative advantage over those proposed in [3], [4], [10] because they take the energy losses into account. Nevertheless, they also utilize a variant of DC power flow equations. A linear MDEP model will provide dependable expansion plans for ADNs only if it incorporates a complete study of the network operation based on AC power flow equations. This issue has recently attracted the attention of some researchers [15], [16]. As an example, the MILP model proposed in [15] employs a linearized version of AC power flow equations to better capture the inherent characteristics of the network. However, this linearized network model is obtained by making several error-prone assumptions that adversely affect its correctness. In [16], a more accurate MILP model reflecting AC power flow equations is developed for the MDEP problem, which utilizes a piecewise-based linearization technique to overcome the nonlinearities. Nevertheless, the accuracy of the adopted linearization technique needs to be improved. In summary, the MILP models proposed in the literature for the MDEP problem sacrifice the accuracy of the network model and, hence, new linear models with higher degrees of accuracy need to be introduced.

From the perspective of Feature 2, several different approaches have been used in the existing literature. Many reported works utilize a deterministic approach in which one or a few certain values are considered for each uncertain parameter [7-11], [16]. In [7-9], for example, all DG units are presumed to be conventional (i.e., no renewable DG units are considered) and the uncertainties associated with loads are completely neglected. In [11], the system demand is characterized by three load levels and the wind power generation is determined based on three given wind speed values that are assumed to remain unchanged during the whole planning horizon. These simplistic approaches will obviously result in inaccurate and unreliable solutions for the MDEP problem as they entirely ignore the uncertainties. Another group of works adopt a scenario-based stochastic programming (SBSP) approach [2-4], [13-15], which models the uncertainties by defining a finite number of scenarios for the random variables and finds the optimal solution of the MDEP problem by weighting the objective function of each scenario in proportion to its probability of occurrence. However, several studies have demonstrated that the SBSP approach is computationally demanding as it requires a large number of scenarios to precisely describe the uncertainties [17]. For example, in [3], [4], a total number of 1296 operating conditions are defined for each planning stage to model the uncertainties associated with renewable DGs and loads. Such a large number of scenarios can obviously cause the MDEP problem to become intractable when dealing with large-scale distribution systems. Probabilistic approaches such as point estimate method (PEM) [1], [18], cumulant method [19], and unscented transformation (UT) method [20] have also attracted the attention of many researchers due to their computational tractability. But the main drawback of these approaches is that they assume the existence of perfect knowledge about the probability distribution functions (PDFs) of random variables, which are very difficult to obtain in practice. For instance, in [1], a two-point estimate method (2-PEM) is utilized to approximate the Gaussian PDF assumed for load demand by two concentration points located around its mean value. The authors of [19] also propose a cumulant-based method to model the uncertainties presuming that the load demand follows a Gaussian distribution and the wind speed has a Weibull distribution. Another approach gaining widespread use is the robust optimization (RO) in which a suitable uncertainty space is defined for uncertain parameters and the optimal solution of the problem is found for the worst-case scenario [21-23]. The RO approach has a low computational demand as opposed to the SBSP approach, and also does not require detailed knowledge about the PDFs of uncertain parameters in contrast to the probabilistic approaches. However, it often leads to over-conservative solutions as it cannot effectively control the degree of conservatism. In summary, despite the efforts of previous researchers, it is essential to develop a more efficient approach that not only is able to adequately characterize the inherent uncertainties of the MDEP problem, but also results in a reasonable computational cost.

In this paper, with respect to Feature 1, first a deterministic non-convex MINLP model is developed for the MDEP problem, which reflects the essential characteristics of the network model in a realistic manner. This model provides several expansion alternatives including construction/replacement of feeder sections, construction/reinforcement of substations, and installation of renewable/conventional DGs. With the aim of obtaining a more tractable problem formulation, the developed non-convex MINLP model is then converted to a convex mixed-integer second-order conic programming (MISOCP) model by proposing a conic quadratic format for AC power flow equations. Finally, a highly accurate polyhedral-based linearization method [24] is utilized to approximate the conic quadratic constraints with a number of linear constraints. This linearization results in an accurate MILP model for the MDEP problem that is computationally tractable and ensures the optimality of the solution found.

With respect to Feature 2, this paper employs a chance-constrained programming (CCP) approach, which is a powerful technique to control the risk in decision making under uncertainty [25]. In this approach, the uncertainties are handled by defining a number of chance constraints (CCs) which ensure that the constraints subject to uncertainty will be satisfied with a certain probability level specified by the decision maker. The only difficulty with using the CCP approach is that the CCs, due to their implicit form, are not straightforward to deal with and, hence, need to be reformulated as explicit constraints. In most of the existing research works (e.g., [26-28]), this reformulation is carried out assuming that the random variables affecting CCs are Gaussian distributed. In practice, however, this assumption is quite unrealistic. Some other works (e.g., [29], [30]) do not consider any specific PDFs for random variables, but they propose approximate reformulations (not exact ones) for CCs, which can adversely affect the correctness and dependability of the CCP approach. To address these issues, we propose a distributionally robust (DR) reformulation for CCs, which not only is exact, but also does not make any assumptions about the uncertainty distributions [31]. To this end, first a moment-based ambiguity set, covering all PDFs whose first two moments lie within its confidence intervals, is constructed. This ambiguity set is then used to derive the DR variants of CCs. After that, using the duality theory of conic linear programming problems [32] and the S-Lemma [33], the DR variants of CCs are equivalently reformulated as a number of explicit nonlinear constraints. Finally, the nonlinear DR reformulations of CCs are expressed in the form of some conic and bilinear constraints that can be linearized using suitable linearization methods.

The main contributions of this paper are as follows:

- Developing a convex MISOCP model with conic quadratic AC power flow equations and employing a highly accurate polyhedral-based linearization method to convert it to an MILP model that guarantees computational tractability and solution optimality for the MDEP problem.
- Proposing a novel distributionally robust chance-constrained (DRCC) model to account for the uncertainties associated with renewable DGs and loads. This model offers four significant advantages: first, it has a low computational demand and provides the opportunity to deal with large-scale systems; second, it requires limited information about the random variables, rather than perfect knowledge of their PDFs; third, it immunizes the solution of the MDEP problem against all realizations of the uncertainty distributions defined within a moment-based ambiguity set; fourth, it enables the decision maker to effectively control the degree of conservatism of the solution. These properties make the proposed DRCC model highly applicable for the planning of ADNs where long-term data about the uncertain parameters are very difficult to acquire.
- Proposing effective linearization techniques to overcome the nonlinearities of the DR reformulations of CCs, resulting in a DRCC-MILP model for the MDEP problem that can be efficiently solved by off-the-shelf optimization tools.

III. Deterministic Problem Formulation

In this section, the uncertainties are ignored and a deterministic mathematical formulation is proposed for the MDEP problem. To this end, first a non-convex MINLP model is developed. This model is then changed to a convex MISOCP model that can be converted to an MILP model using a highly accurate linearization method. The key advantage of the proposed MILP model is that it can be solved using standard off-the-shelf mathematical programming solvers that not only guarantee convergence to the global optimal solution, but also provide a measure of the distance to the global optimum during the solution process.

A. Non-Convex MINLP Model of the MDEP Problem

This model, which is partly based on the models described in [11] and [16], provides several expansion alternatives while minimizing the total investment and operation costs and taking all the necessary constraints into account, as given in (1)-(44).

1) Objective Function

$$\text{Minimize } \; c = c^{Inv.} + c^{Oper.} \tag{1}$$

$$c^{Inv.} = \sum_{t\in\Omega^T} \frac{1}{(1+r)^{(t-1)D}} \Big[\sum_{(ij)\in\Omega^{FR}} \sum_{a\in\left(\Omega^a - a_{ij}^{FR}\right)} c_a^{FR} l_{ij} x_{ij,a,t}^{FR} + \sum_{(ij)\in\Omega^{FC}} \sum_{a\in\Omega^a} c_a^{FC} l_{ij} x_{ij,a,t}^{FC} + \sum_{i\in\Omega^{SR}} \sum_{b\in\Omega^b} c_b^{SR} x_{i,b,t}^{SR} + \sum_{i\in\Omega^{SC}} \sum_{b\in\Omega^b} c_b^{SC} x_{i,b,t}^{SC} + \sum_{i\in\left(\Omega^{NG}\cap\Omega_t^{NL}\right)} \sum_{g\in\Omega^{gr}} c_g^{GR} x_{i,g,t}^{GR} + \sum_{i\in\left(\Omega^{NG}\cap\Omega_t^{NL}\right)} \sum_{g\in\Omega^{gc}} c_g^{GC} x_{i,g,t}^{GC} \Big] \tag{2}$$

$$c^{Oper.} = \sum_{t\in\Omega^T} \frac{1}{(1+r)^{(t-1)D}} \frac{(1+r)^D - 1}{r(1+r)^D} \Big[\sum_{i\in\Omega^S} \tau c^E P_{i,t}^S + \sum_{i\in\Omega^S} \tau c_i^{SO} \phi^S f_{i,t}^S + \sum_{i\in\left(\Omega^{NG}\cap\Omega_t^{NL}\right)} \sum_{g\in\Omega^{gc}} \tau c_g^{EGC} P_{i,g,t}^{GC} \Big] \tag{3}$$

The objective function is comprised of two parts. In equation (2), $c^{Inv.}$ represents the present value of the investment costs required for replacement and construction of feeder sections, reinforcement and construction of substations, and installation of renewable and conventional DGs. In equation (3), $c^{Oper.}$ represents the present value of the system operation costs including the cost of electrical energy received from the upstream power grid, operation costs of substations, and generation costs of conventional DGs. Note that $c^{Oper.}$ also includes the costs of energy losses in feeder sections; this is because the active power received from the upstream grid (i.e., $P_{i,t}^{S}$) includes the power losses in feeder sections as well.

2) Constraints

$$\sum_{(ki)\in\Omega^F}\sum_{a\in\Omega^a}\left[P_{ki,a,t}^F - R_a l_{ki} f_{ki,a,t}^F\right] - \sum_{(ij)\in\Omega^F}\sum_{a\in\Omega^a} P_{ij,a,t}^F + P_{i,t}^S + \sum_{g\in\Omega^{gc}} P_{i,g,t}^{GC} + \sum_{g\in\Omega^{gr}} P_{i,g,t}^{GR} = \overline{\overline{P_{i,t}^{D}}} \quad \forall i \in \Omega^N, \forall t \in \Omega^T \quad (4)$$

$$\sum_{(ki)\in\Omega^F}\sum_{a\in\Omega^a}\left[Q_{ki,a,t}^F - X_a l_{ki} f_{ki,a,t}^F\right] - \sum_{(ij)\in\Omega^F}\sum_{a\in\Omega^a} Q_{ij,a,t}^F + Q_{i,t}^S + \sum_{g\in\Omega^{gc}} Q_{i,g,t}^{GC} + \sum_{g\in\Omega^{gr}} Q_{i,g,t}^{GR} = \overline{\overline{Q_{i,t}^{D}}} \quad \forall i \in \Omega^N, \forall t \in \Omega^T \quad (5)$$

$$u_{i,t} - u_{j,t} = \sum_{a\in\Omega^a}\left[2\left(R_a l_{ij} P_{ij,a,t}^F + X_a l_{ij} Q_{ij,a,t}^F\right) - \left(Z_a l_{ij}\right)^2 f_{ij,a,t}^F\right] + \Delta V_{ij,t} \quad \forall (ij) \in \Omega^F, \forall t \in \Omega^T \quad (6)$$

$$u_{i,t}\hat{f}_{ij,t}^F = \left(\hat{S}_{ij,t}^F\right)^2 \quad \forall (ij) \in \Omega^F, \forall t \in \Omega^T \quad (7)$$

$$\left(\hat{S}_{ij,t}^F\right)^2 = \left(\hat{P}_{ij,t}^F\right)^2 + \left(\hat{Q}_{ij,t}^F\right)^2 \quad \forall (ij) \in \Omega^F, \forall t \in \Omega^T \quad (8)$$

$$\hat{f}_{ij,t}^F = \sum_{a\in\Omega^a} f_{ij,a,t}^F \quad \forall (ij) \in \Omega^F, \forall t \in \Omega^T \quad (9)$$

$$\hat{P}_{ij,t}^F = \sum_{a\in\Omega^a} P_{ij,a,t}^F \quad \forall (ij) \in \Omega^F, \forall t \in \Omega^T \quad (10)$$

$$\hat{Q}_{ij,t}^F = \sum_{a\in\Omega^a} Q_{ij,a,t}^F \quad \forall (ij) \in \Omega^F, \forall t \in \Omega^T \quad (11)$$

$$\hat{S}_{ij,t}^F = \sum_{a\in\Omega^a} S_{ij,a,t}^F \quad \forall (ij) \in \Omega^F, \forall t \in \Omega^T \quad (12)$$

$$u_{i,t} f_{i,t}^S = \left(S_{i,t}^S\right)^2 \quad \forall i \in \Omega^S, \forall t \in \Omega^T \quad (13)$$

$$\left(S_{i,t}^S\right)^2 = \left(P_{i,t}^S\right)^2 + \left(Q_{i,t}^S\right)^2 \quad \forall i \in \Omega^S, \forall t \in \Omega^T \quad (14)$$

$$\left(\underline{V}\right)^2 \le u_{i,t} \le \left(\overline{V}\right)^2 \quad \forall i \in \Omega^N, \forall t \in \Omega^T \quad (15)$$

$$f_{ij,a,t}^F \le \left(\overline{I_a}\right)^2 y_{ij,a,t} \quad \forall (ij) \in \Omega^F, a \in \Omega^a, \forall t \in \Omega^T \quad (16)$$

$$\left|\Delta V_{ij,t}\right| \le \overline{\Delta V}\left(1 - \sum_{a\in\Omega^a} y_{ij,a,t}\right) \quad \forall (ij) \in \Omega^F, \forall t \in \Omega^T \quad (17)$$

$$S_{i,t}^S \le \overline{S_i^0} + \sum_{v=1}^{t}\sum_{b\in\Omega^b} \overline{S_b}\, x_{i,b,v}^{SR} \quad \forall i \in \Omega^{SR}, \forall t \in \Omega^T \quad (18)$$

$$S_{i,t}^S \le \sum_{v=1}^{t}\sum_{b\in\Omega^b} \overline{S_b}\, x_{i,b,v}^{SC} \quad \forall i \in \Omega^{SC}, \forall t \in \Omega^T \quad (19)$$

$$0 \le P_{i,g,t}^{GC} \le \overline{P_g^{GC}} x_{i,g,t}^{GC} \quad \forall i \in (\Omega^{NG} \cap \Omega_t^{NL}), g \in \Omega^{gc}, \forall t \in \Omega^T \quad (20)$$

$$\left|Q_{i,g,t}^{GC}\right| \le \overline{Q_g^{GC}}\, x_{i,g,t}^{GC} \quad \forall i \in (\Omega^{NG} \cap \Omega_t^{NL}), g \in \Omega^{gc}, \forall t \in \Omega^T \quad (21)$$

$$P_{i,g,t}^{GR} = \overline{\overline{P_g^{GR}}} x_{i,g,t}^{GR} \quad \forall i \in (\Omega^{NG} \cap \Omega_t^{NL}), g \in \Omega^{gr}, \forall t \in \Omega^T \quad (22)$$

$$Q_{i,g,t}^{GR} = \tan\left(\cos^{-1}(\rho^{GR})\right)\overline{\overline{P_g^{GR}}} x_{i,g,t}^{GR} \quad \forall i \epsilon (\Omega^{NG} \cap \Omega_t^{NL}), g \epsilon \Omega^{gr}, \forall t \epsilon \Omega^T \quad (23)$$

$$\sum_{t\in\Omega^T}\sum_{a\in\Omega^a} x_{ij,a,t}^{FC} \le 1 \quad \forall (ij) \in \Omega^{FC} \quad (24)$$

$$\sum_{t\in\Omega^T}\sum_{a\in\left(\Omega^a - a_{ij}^{FR}\right)} x_{ij,a,t}^{FR} \le 1 \quad \forall (ij) \in \Omega^{FR} \quad (25)$$

$$\sum_{t\in\Omega^T}\sum_{b\in\Omega^b} x_{i,b,t}^{SC} \le 1 \quad \forall i \in \Omega^{SC} \quad (26)$$

$$\sum_{t\in\Omega^T}\sum_{b\in\Omega^b} x_{i,b,t}^{SR} \le 1 \quad \forall i \in \Omega^{SR} \quad (27)$$

$$\sum_{t\in\Omega^T}\sum_{g\in\Omega^{gc}} x_{i,g,t}^{GC} + \sum_{t\in\Omega^T}\sum_{g\in\Omega^{gr}} x_{i,g,t}^{GR} \le 1 \quad \forall i \in \Omega^{NG} \quad (28)$$

$$\sum_{t\in\Omega^T}\sum_{i\in\left(\Omega^{NG}\cap\Omega_t^{NL}\right)}\sum_{g\in\Omega^{gr}} x_{i,g,t}^{GR} \le \overline{N^{GR}} \quad (29)$$

$$\sum_{t\in\Omega^T}\sum_{i\in\left(\Omega^{NG}\cap\Omega_t^{NL}\right)}\sum_{g\in\Omega^{gc}} x_{i,g,t}^{GC} \le \overline{N^{GC}} \quad (30)$$

$$y_{ij,a,t} \le \sum_{v=1}^{t} x_{ij,a,v}^{FR} \quad \forall (ij) \in \Omega^{FR}, \forall a \in \left(\Omega^a - a_{ij}^{FR}\right), \forall t \in \Omega^T \quad (31)$$

$$y_{ij,a,t} \le 1 - \sum_{v=1}^{t}\sum_{\omega\in\left(\Omega^a - a_{ij}^{FR}\right)} x_{ij,\omega,v}^{FR} \quad \forall (ij) \epsilon \Omega^{FR}, \forall a = a_{ij}^{FR}, \forall t \epsilon \Omega^T \quad (32)$$

$$y_{ij,a,t} = 0 \quad \forall (ij) \in \Omega^{FI}, \forall a \in \left(\Omega^a - a_{ij}^{FI}\right), \forall t \in \Omega^T \quad (33)$$

$$y_{ij,a,t} \le 1 \quad \forall (ij) \in \Omega^{FI}, \forall a = a_{ij}^{FI}, \forall t \in \Omega^T \quad (34)$$

$$y_{ij,a,t} \le \sum_{v=1}^{t} x_{ij,a,v}^{FC} \quad \forall (ij) \in \Omega^{FC}, \forall a \in \Omega^a, \forall t \in \Omega^T \quad (35)$$

$$\sum_{(ij)\in\Omega^F}\sum_{a\in\Omega^a} y_{ij,a,t} = |\Omega^N| - |\Omega^{NS}| - \sum_{i\in\Omega_t^{NT}}\left(1 - z_{i,t}\right) \quad \forall t \epsilon \Omega^T \quad (36)$$

$$\sum_{a\in\Omega^a} y_{ki,a,t} \le z_{i,t} \quad \forall (ki) \in \Omega^F, \forall i \in \Omega_t^{NT}, \forall t \in \Omega^T \quad (37)$$

$$\sum_{a\in\Omega^a} y_{ij,a,t} \le z_{i,t} \quad \forall (ij) \in \Omega^F, \forall i \in \Omega_t^{NT}, \forall t \in \Omega^T \quad (38)$$

$$\sum_{(ki)\in\Omega^F}\sum_{a\in\Omega^a} y_{ki,a,t} + \sum_{(ij)\in\Omega^F}\sum_{a\in\Omega^a} y_{ij,a,t} \ge 2 z_{i,t} \quad \forall i \epsilon \Omega_t^{NT}, \forall t \epsilon \Omega^T \quad (39)$$

$$\sum_{(ki)\in\Omega^F} \tilde{\theta}_{ki,t}^F - \sum_{(ij)\in\Omega^F} \tilde{\theta}_{ij,t}^F + \tilde{\theta}_{i,t}^S = \tilde{\theta}_{i,t}^D \quad \forall i \in \Omega^N, \forall t \in \Omega^T \quad (40)$$

$$0 \le \tilde{\theta}_{ij,t}^F \le |\Omega^{NG}| \sum_{a\in\Omega^a} y_{ij,a,t} \quad \forall (ij) \in \Omega^F, \forall t \in \Omega^T \quad (41)$$

$$0 \le \tilde{\theta}_{i,t}^S \le |\Omega^{NG}| \quad \forall i \in \Omega^{SR}, \forall t \in \Omega^T \quad (42)$$

$$0 \le \tilde{\theta}_{i,t}^S \le |\Omega^{NG}|\left(\sum_{v=1}^{t}\sum_{b\in\Omega^b} x_{i,b,v}^{SC}\right) \quad \forall i \in \Omega^{SC}, \forall t \in \Omega^T \quad (43)$$

$$\tilde{\theta}_{i,t}^D = \begin{cases} 1 & \forall i \in (\Omega^{NG} \cap \Omega_t^{NL}), \forall t \in \Omega^T \\ 0 & \forall i \notin (\Omega^{NG} \cap \Omega_t^{NL}), \forall t \in \Omega^T \end{cases} \quad (44)$$

The above constraints can be categorized into four main groups:

a) Power flow equations: Constraints (4)-(14) represent the AC power flow model in a radial distribution network based on a set of recursive equations called *DistFlow branch equations* [34-36]. More specifically, constraints (4) and (5) ensure the active and reactive power balances in system nodes. Equations (6)-(8) relate the active, reactive, and apparent power flows and the current flow of a feeder selction to the voltages of its sending and receiving ends. These three equations apply Kirchhoff's voltage law (KVL) to each feeder section. Constraints (9)-(12) are employed based on the fact that each feeder section uses only one of the candidate conductor types at each planning stage. Constraints (13) and (14) relate the active, reactive, and apparent powers provided by a substation to its current flow and voltage. Note that *DistFlow branch equations* are an exact representation of the AC power flow equations in a radial distribution network [34-36]. The detailed proof of this exactness can be found in [35], [36].

b) Voltage, current, and capacity limits: Constraint (15) determines the acceptable range of the nodal voltage magnitudes. Constraint (16) represents the limits on the current flows of feeder sections based on the conductor types used for constructing them. Constraint (17) sets appropriate bounds on the variable $\Delta V_{ij,t}$ used in (6). Constraints (18) and (19) cause the apparent power provided by each substation to be less than its installed capacity. Constraints (20) and (21) limit the active and reactive powers generated by conventional DGs. Constraints (22) and (23) set the active and reactive power generations of renewable DGs equal to their expected values. Note that renewable DGs are assumed to operate at a constant power factor (ρ^{GR}) as they often lack the ability to provide controlled reactive power.

c) Constraints on binary investment and utilization variables: Constraints (24)-(27) ensure that a maximum of one construction or reinforcement is performed for each feeder section or substation during the planning horizon. Constraint (28) limits the number of DG installations at each candidate node to one. Constraints (29) and (30) specify the maximum number of renewable and conventional DGs that can be installed in the system. Constraints (31)-(35) address the operating conditions of different feeder section categories including existing replaceable/irreplaceable feeder sections and candidate feeder sections for construction. In this regard, $y_{ij,a,t}$ equals one if its corresponding feeder section is operated and zero otherwise. Imposing these constraints on the utilization variables denoted by "y" guarantees that a feeder section with a specific conductor type can be used only if its corresponding investment has already been made.

d) Radiality constraints: Constraints (36)-(44) guarantee the radiality of the distribution network [11], [37]. When DGs are not considered as expansion alternatives, (36)-(39) are sufficient to ensure the radiality. However, when DGs are brought into play, (40)-(44) should also be considered to prevent the existence of areas exclusively supplied by DGs. These constraints assign fictitious current flow demands to the candidate nodes for DG installation and, in this way, keep them connected to the substations to preclude formation of isolated areas [11]. Moreover, the distribution system is here assumed to include a number of so-called *transfer nodes* at some of the planning stages [37]. These nodes are not connected to the loads or substations, but they can be used to connect different load nodes to each other and, in this way, may help to find better planning solutions. The binary variables denoted by "z" indicate the operating conditions of the transfer nodes, so that $z_{i,t}$ equals one if its corresponding transfer node is utilized and zero otherwise.

B. Convex MISOCP Model Proposed for the MDEP Problem

Although the above-discussed model well reflects the essential characteristics of the MDEP problem, it is a non-convex MINLP model that not only is very difficult to solve, but also cannot guarantee obtaining the global optimal solution. To overcome these drawbacks, it should be changed to a convex model.

The non-convexity of the model arises from (7), (8), (13), and (14). In order to convexify the model, first the objective function should be modified in the following manner:

$$c = c^{Inv.} + c^{Oper.} + c^{Conv.} \tag{45}$$

$$c^{Conv.} = \partial \left[\sum_{t\in\Omega^T}\sum_{(ij)\in\Omega^F}\hat{S}^F_{ij,t} + \sum_{t\in\Omega^T}\sum_{i\in\Omega^S}S^S_{i,t} + \sum_{(ij)\in\Omega^F}\sum_{a\in\Omega^a}f^F_{ij,a,t}\right] \tag{46}$$

The main purpose of this modification is to add positive multiples of the variables $\hat{S}^F_{ij,t}$ and $S^S_{i,t}$ to the objective function. Accordingly, ∂ is a positive coefficient that can be set to a small value such as 10^{-6}. Considering the modified objective function, convexity can now be obtained by relaxing the equality constraints (7), (8), (13), and (14) as follows:

$$\left(\hat{S}^F_{ij,t}\right)^2 \geq \left(\hat{P}^F_{ij,t}\right)^2 + \left(\hat{Q}^F_{ij,t}\right)^2 \quad \forall (ij)\in\Omega^F, \forall t\in\Omega^T \tag{47}$$

$$\left(S^S_{i,t}\right)^2 \geq \left(P^S_{i,t}\right)^2 + \left(Q^S_{i,t}\right)^2 \quad \forall i\in\Omega^S, \forall t\in\Omega^T \tag{48}$$

$$u_{i,t}\hat{f}^F_{ij,t} \geq \left(\hat{S}^F_{ij,t}\right)^2 \quad \forall (ij)\in\Omega^F, \forall t\in\Omega^T \tag{49}$$

$$u_{i,t}f^S_{i,t} \geq \left(S^S_{i,t}\right)^2 \quad \forall i\in\Omega^S, \forall t\in\Omega^T \tag{50}$$

Note that the above relaxation technique is exact and hence the inequality constraints (47)-(50) act exactly as equality constraints. The detailed proof of the exactness of this relaxation technique can be found in [38]. Based on [38], the proposed relaxation technique will be exact if: 1) the network is radial; and 2) the objective function is strictly increasing with respect to $\hat{S}^F_{ij,t}$, $S^S_{i,t}$, $\hat{f}^F_{ij,t}$, and $f^S_{i,t}$, which appear on the left-hand sides of (47)-(50), respectively. It is obvious that the first condition is fully satisfied because the radiality constraints force the network to always be radial. To satisfy the second condition, however, the objective function should contain positive multiples of $\hat{S}^F_{ij,t}$, $S^S_{i,t}$, $\hat{f}^F_{ij,t}$, and $f^S_{i,t}$. A careful look at the objective function reveals that it already includes positive multiples of $f^S_{i,t}$, but it does not contain $\hat{S}^F_{ij,t}$, $S^S_{i,t}$, and $\hat{f}^F_{ij,t}$. Therefore, the new component (46) is included in the objective function to make it strictly increasing with respect to $\hat{S}^F_{ij,t}$, $S^S_{i,t}$, and $\hat{f}^F_{ij,t}$ as required by the second condition.

Using the above relaxation technique, the resultant MDEP model is now a convex MISOCP problem that, in contrast to the initial non-convex MINLP problem, is tractable and ensures obtaining the global optimal solution. However, it is still computationally demanding due to the nonlinearities of (47)-(50). Therefore, these four constraints should also be linearized.

C. Proposed MILP Model for the MDEP Problem

As the first step to overcome the nonlinearities, (47) and (48) are rewritten in the following manner:

$$\hat{S}^F_{ij,t} \geq \sqrt{\left(\hat{P}^F_{ij,t}\right)^2 + \left(\hat{Q}^F_{ij,t}\right)^2} \quad \forall (ij)\in\Omega^F, \forall t\in\Omega^T \tag{51}$$

$$S^S_{i,t} \geq \sqrt{\left(P^S_{i,t}\right)^2 + \left(Q^S_{i,t}\right)^2} \quad \forall i\in\Omega^S, \forall t\in\Omega^T \tag{52}$$

The left-hand sides of (49) and (50) can also be expressed as:

$$u_{i,t}\hat{f}^F_{ij,t} = \left[\left(u_{i,t}+\hat{f}^F_{ij,t}\right)/2\right]^2 - \left[\left(u_{i,t}-\hat{f}^F_{ij,t}\right)/2\right]^2 \tag{53}$$

$$u_{i,t}f^S_{i,t} = \left[\left(u_{i,t}+f^S_{i,t}\right)/2\right]^2 - \left[\left(u_{i,t}-f^S_{i,t}\right)/2\right]^2 \tag{54}$$

As a result, (49) and (50) can be written as:

$$\left[\left(u_{i,t}+\hat{f}^F_{ij,t}\right)/2\right] \geq \sqrt{\left[\left(u_{i,t}-\hat{f}^F_{ij,t}\right)/2\right]^2 + \left(\hat{S}^F_{ij,t}\right)^2} \quad \forall (ij)\epsilon\Omega^F, \forall t\epsilon\Omega^T \tag{55}$$

$$\left[\left(u_{i,t}+f^S_{i,t}\right)/2\right] \geq \sqrt{\left[\left(u_{i,t}-f^S_{i,t}\right)/2\right]^2 + \left(S^S_{i,t}\right)^2} \quad \forall i\epsilon\Omega^S, \forall t\epsilon\Omega^T \tag{56}$$

In this way, (47)-(50) are respectively represented as the second-order conic constraints (51), (52), (55), and (56), which all have the following form:

$$x_3 \geq \sqrt{(x_1)^2 + (x_2)^2} \tag{57}$$

Using a highly accurate method based on polyhedral approximation, the second-order conic constraint (57) can be approximated by a system of linear equalities and inequalities that are expressed in terms of x_1, x_2, x_3, and a number of auxiliary variables (i.e., ξ_ℓ and η_ℓ) [24]:

$$\xi_\ell \geq |x_1|\ , \quad \eta_\ell \geq |x_2| \qquad \forall \ell = 0 \tag{58}$$

$$\begin{cases} \xi_\ell = \xi_{\ell-1}\cos\left(\frac{\pi}{2^{\ell+1}}\right) + \eta_{\ell-1}\sin\left(\frac{\pi}{2^{\ell+1}}\right) \\ \eta_\ell \geq \left|-\xi_{\ell-1}\sin\left(\frac{\pi}{2^{\ell+1}}\right) + \eta_{\ell-1}\cos\left(\frac{\pi}{2^{\ell+1}}\right)\right| \end{cases} \quad \forall \ell = 1, \dots, \mathcal{L} \tag{59}$$

$$\xi_\ell \leq x_3 \quad , \quad \eta_\ell \leq \xi_\ell \tan\left(\frac{\pi}{2^{\ell+1}}\right) \qquad \forall \ell = \mathcal{L} \tag{60}$$

Note that $\mathcal{L}$ is a parameter that determines the number of additional constraints and variables required to linearize (57), and the linearization error will decrease as this parameter increases. In [24], it is proved that the set of linear constraints (58)-(60) approximate (57) in such a way that:

$$x_3(1+\varrho) \geq \sqrt{(x_1)^2 + (x_2)^2} \tag{61}$$

where ϱ is dependent on $\mathcal{L}$ and can be calculated as follows:

$$\varrho = \left[1/\cos\left(\frac{\pi}{2^{\mathcal{L}+1}}\right)\right] - 1 \tag{62}$$

Choosing an appropriate value for $\mathcal{L}$ will obviously result in a highly accurate approximation. For instance, choosing $\mathcal{L} = 8$ leads to $\varrho = 1.88 \times 10^{-5}$, which demonstrates the high accuracy of the polyhedral approximation.

In a similar manner, each of the conic quadratic constraints (51), (52), (55), and (56) can also be replaced by the polyhedral approximation represented by (58)-(60). This causes the MISOCP model to be converted to an MILP model.

IV. DISTRIBUTIONALLY ROBUST CHANCE-CONSTRAINED PROBLEM FORMULATION

In this section, the developed deterministic MILP model is improved to incorporate the uncertainties of renewable DGs and loads. In this regard, first a number of CCs are added to the model to guarantee that the constraints subject to uncertainty will be satisfied with a certain probability level. These CCs are then reformulated as a number of explicit nonlinear constraints that are robust against the PDFs of random variables. Finally, the nonlinear DR reformulations proposed for CCs are linearized using appropriate techniques.

A. Chance Constraints

The operational constraints of power systems are of two types: hard and soft [39]. Hard constraints (e.g., power balance equations and power generation limits) are physically impossible to violate as they are imposed by the nature of the system. Whereas, minor violations of soft constraints (e.g., voltage and current magnitude limits) for short time periods are quite tolerable. Note that the CCs can only be applied to soft constraints. Considering this fact, we have added the following CCs to the proposed deterministic MILP model to account for the uncertainties associated with renewable generations and loads:

$$\mathbb{P}\left\{\left(\underline{V}\right)^2 \leq \tilde{u}_{i,t}(\tilde{\boldsymbol{\chi}}) \leq \left(\overline{V}\right)^2\right\} \geq 1-\epsilon \quad \forall i\in\Omega^N, \forall t\in\Omega^T \tag{63}$$

$$\mathbb{P}\left\{\tilde{f}^F_{ij,a,t}(\tilde{\boldsymbol{\chi}}) \leq \left(\overline{I_a}\right)^2 y_{ij,a,t}\right\} \geq 1-\epsilon \quad \forall (ij)\epsilon\Omega^F, a\epsilon\Omega^a, \forall t\epsilon\Omega^T \tag{64}$$

$$\mathbb{P}\left\{\tilde{S}^S_{i,t}(\tilde{\boldsymbol{\chi}}) \leq \overline{S^0_i} + \sum_{\upsilon=1}^{t}\sum_{b\in\Omega^b}\overline{S_b}\, x^{SR}_{i,b,\upsilon}\right\} \geq 1-\epsilon \quad \forall i\epsilon\Omega^{SR}, \forall t\epsilon\Omega^T \tag{65}$$

$$\mathbb{P}\left\{\tilde{S}^S_{i,t}(\tilde{\boldsymbol{\chi}}) \leq \sum_{\upsilon=1}^{t}\sum_{b\in\Omega^b}\overline{S_b}\, x^{SC}_{i,b,\upsilon}\right\} \geq 1-\epsilon \quad \forall i\in\Omega^{SC}, \forall t\in\Omega^T \tag{66}$$

where $\tilde{\boldsymbol{\chi}} = \langle\widetilde{\chi_1}, \widetilde{\chi_2}\rangle = \langle\widetilde{\chi^{GR}}, \widetilde{\chi^{D}}\rangle$ is a vector containing two random variables defined to characterize the stochasticity of renewable generations and loads; and $\tilde{u}_{i,t}(\tilde{\boldsymbol{\chi}})$, $\tilde{f}^F_{ij,a,t}(\tilde{\boldsymbol{\chi}})$, and $\tilde{S}^S_{i,t}(\tilde{\boldsymbol{\chi}})$ are the stochastic equivalents of the variables $u_{i,t}$, $f_{ij,a,t}^{F}$, and $S_{i,t}^{S}$, respectively. The above CCs ensure that the voltage magnitudes of nodes, current flows of feeder sections, and apparent powers of substations remain within their bounds with a probability of at least $1-\epsilon$, where ϵ is a controllable risk parameter that enables the decision maker to adjust the degree of conservatism of the solution. It is clear that decreasing the value of ϵ results in more conservative solutions for the MDEP problem.

Unfortunately, (63)-(66) are very challenging to handle due to their implicit form. The implicitness of these CCs arises from the fact that evaluation of the probability statements given on their left-hand sides is not straightforward as the PDFs of $\widetilde{\chi^{GR}}$ and $\widetilde{\chi^{D}}$ are not perfectly known. Most of the existing research works using the CCP approach (e.g., [26-28]) assume that the random variables follow a Gaussian distribution and, based on this unrealistic assumption, reformulate the CCs as a number of explicit constraints. In this paper, however, a novel method is proposed to reformulate CCs, which does not make any assumption about the PDF types of the random variables [31]. That is, we obtain the explicit counterparts of CCs in such a way that their satisfaction is guaranteed irrespective of the PDF types of the random variables. In this way, CCs are immunized against the probability distributions of the random variables. Based on this fact, the proposed method is called "distributionally robust", which means "robust with respect to probability distributions". In the following, the DR reformulation proposed for CCs is described in detail.

B. DR Reformulation of CCs

In order to simplify the notation, each of the constraints (63)-(66) can be expressed as:

$$\mathbb{P}\{\widetilde{H}(\widetilde{\boldsymbol{\chi}}) \le K\} \ge 1-\epsilon \tag{67}$$

where $\widetilde{H}(\widetilde{\boldsymbol{\chi}})$ represents the stochastic variables $\tilde{u}_{i,t}(\widetilde{\boldsymbol{\chi}})$, $\tilde{f}_{ij,a,t}^{F}(\widetilde{\boldsymbol{\chi}})$, and $\tilde{S}_{i,t}^{S}(\widetilde{\boldsymbol{\chi}})$; and K is a variable representing the remaining part of each CC. On the other hand, $\widetilde{H}(\widetilde{\boldsymbol{\chi}})$ can be defined as an affine function of $\widetilde{\boldsymbol{\chi}}$ (see [40], [41]):

$$\widetilde{H}(\widetilde{\boldsymbol{\chi}}) = H + \textstyle\sum_{n=1}^{2} A_n \widetilde{\chi_n} = H + \boldsymbol{A}^T \widetilde{\boldsymbol{\chi}} \tag{68}$$

where H represents the deterministic part of $\widetilde{H}(\widetilde{\boldsymbol{\chi}})$; A_1 and A_2 are the affine coefficients of $\widetilde{\chi_1}$ and $\widetilde{\chi_2}$, respectively; and $\boldsymbol{A} = \langle A_1, A_2\rangle$ is the vector of affine coefficients.

As a result, by defining $B = K - H$, (67) can be rewritten in the following form:

$$\mathbb{P}\{\boldsymbol{A}^T \widetilde{\boldsymbol{\chi}} \le B\} \ge 1-\epsilon \tag{69}$$

Now, we describe how to derive the DR reformulation of (69). First, a moment-based ambiguity set ($\mathcal{D}$) is built to specify all PDFs for which the satisfaction of (69) must be guaranteed [31]:

$$\mathcal{D} = \left\{ f(\widetilde{\boldsymbol{\chi}}) \middle| \begin{array}{l} \int_{\widetilde{\boldsymbol{\chi}}\in\mathbb{S}} f(\widetilde{\boldsymbol{\chi}}) d\widetilde{\boldsymbol{\chi}} = 1 \\ \underline{\mu_n} \le \mathbb{E}[\tilde{\chi}_n] \le \overline{\mu_n} \quad \forall n = 1,2 \\ \underline{\sigma_n} \le \mathbb{E}[(\tilde{\chi}_n)^2] \le \overline{\sigma_n} \quad \forall n = 1,2 \end{array} \right\} \tag{70}$$

where $f(\widetilde{\boldsymbol{\chi}})$ is the PDF of $\widetilde{\boldsymbol{\chi}}$; $\mathbb{S} \in \mathbb{R}^2$ is the support of $f(\widetilde{\boldsymbol{\chi}})$; $[\underline{\mu_n}, \overline{\mu_n}]$ is the confidence interval of the first moment of the nth random variable; and $[\underline{\sigma_n}, \overline{\sigma_n}]$ is the confidence interval of the second moment of nth random variable. The three conditions $\mathcal{D}$ ensure that: (i) the integral of $f(\widetilde{\boldsymbol{\chi}})$ over its support is equal to one; (ii) the first moment of $\tilde{\chi}_n$ lies in the determined interval; and (iii) the second moment of $\tilde{\chi}_n$ falls within the specified range. Note that $\mathcal{D}$ covers all PDFs whose first and second moments agree with its conditions and, hence, it can be used to define a huge family of uncertainty distributions. Considering this ambiguity set, the DR variant of (69) can be obtained as follows:

$$\inf_{f(\widetilde{\boldsymbol{\chi}})\in\mathcal{D}} \mathbb{P}\{\boldsymbol{A}^T \widetilde{\boldsymbol{\chi}} \le B\} \ge 1-\epsilon \tag{71}$$

The left-hand side of (71) yields the worst-case probability bound of $\mathbb{P}\{\boldsymbol{A}^T \widetilde{\boldsymbol{\chi}} \le B\}$ over $\mathcal{D}$ and is equal to the objective value of the following optimization problem:

$$\varGamma = \min_{f(\widetilde{\boldsymbol{\chi}})} \int_{\widetilde{\boldsymbol{\chi}}\in\mathbb{S}} \mathbb{I}_{\mathcal{C}}(\widetilde{\boldsymbol{\chi}}) f(\widetilde{\boldsymbol{\chi}}) d\widetilde{\boldsymbol{\chi}} \tag{72}$$

$$\text{s.t.} \quad \int_{\widetilde{\boldsymbol{\chi}}\in\mathbb{S}} f(\widetilde{\boldsymbol{\chi}}) d\widetilde{\boldsymbol{\chi}} = 1 \tag{73}$$

$$\underline{\mu_n} \le \int_{\widetilde{\boldsymbol{\chi}}\in\mathbb{S}} \tilde{\chi}_n f(\widetilde{\boldsymbol{\chi}}) d\widetilde{\boldsymbol{\chi}} \le \overline{\mu_n} \quad \forall n = 1,2 \tag{74}$$

$$\underline{\sigma_n} \le \int_{\widetilde{\boldsymbol{\chi}}\in\mathbb{S}} (\tilde{\chi}_n)^2 f(\widetilde{\boldsymbol{\chi}}) d\widetilde{\boldsymbol{\chi}} \le \overline{\sigma_n} \quad \forall n = 1,2 \tag{75}$$

where $\mathbb{I}_{\mathcal{C}}(\widetilde{\boldsymbol{\chi}})$ is the indicator function over the set $\mathcal{C} = \{\widetilde{\boldsymbol{\chi}} | \boldsymbol{A}^T \widetilde{\boldsymbol{\chi}} \le B\}$; that is, $\mathbb{I}_{\mathcal{C}}(\widetilde{\boldsymbol{\chi}}) = 1$ if $\widetilde{\boldsymbol{\chi}} \in \varLambda$ and $\mathbb{I}_{\mathcal{C}}(\widetilde{\boldsymbol{\chi}}) = 0$ otherwise. Obviously, (71) will be satisfied when $\varGamma \ge 1-\epsilon$. In [31], it is demonstrated that by applying the duality theory of conic linear programming problems [32] to the optimization problem (72)-(75) and using the S-Lemma [33], (71) can be equivalently reformulated as follows:

$$q + \textstyle\sum_{n=1}^{2} \left(\underline{\mu_n}\, p_n^L - \overline{\mu_n}\, p_n^U\right) + \sum_{n=1}^{2} \left(\underline{\sigma_n}\, h_n^L - \overline{\sigma_n}\, h_n^U\right) \ge 1-\epsilon \tag{76}$$

$$q + \textstyle\sum_{n=1}^{2} \alpha_n \le 1 \tag{77}$$

$$q + \textstyle\sum_{n=1}^{2} \beta_n \le \varUpsilon B \tag{78}$$

$$\left\| \begin{bmatrix} p_n^L - p_n^U \\ \alpha_n + h_n^L - h_n^U \end{bmatrix} \right\| \le \alpha_n - h_n^L + h_n^U \qquad \forall n = 1,2 \tag{79}$$

$$\left\| \begin{bmatrix} p_n^L - p_n^U + \varUpsilon A_n \\ \beta_n + h_n^L - h_n^U \end{bmatrix} \right\| \le \beta_n - h_n^L + h_n^U \qquad \forall n = 1,2 \tag{80}$$

where $q, p_n^L, p_n^U, h_n^L, h_n^U, \alpha_n, \beta_n, \varUpsilon \ge 0$ are auxiliary variables.

By deriving (76)-(80), the DR reformulation of (69) over $\mathcal{D}$ is now achieved. In other words, utilization of (76)-(80) guarantees that (69) will be satisfied for all PDFs covered by $\mathcal{D}$. It is worthwhile to note that (76) explicitly includes the risk parameter ϵ. As a result, the proposed DRCC programming approach is able to directly control the robustness level of the solution based on the value chosen for the risk parameter ϵ. This ability to directly control the robustness level prevents the proposed DRCC programming approach from resulting in over-conservative solutions.

However, (78)-(80) are highly nonlinear and make the MDEP problem intractable. To address this issue, the nonlinearities of the noted constraints must be eliminated.

C. Linearization of the Proposed DR Reformulation

In the following, (78)-(80) are linearized to attain a tractable DRCC-MILP model for the MDEP problem.

1) Linearization of Constraint (78)

The nonlinearity of this constraint is only due to the bilinear term $\varUpsilon B$ on its right-hand side. This bilinear term can be rewritten as follows:

$$\varUpsilon B = [(B+\varUpsilon)/2]^2 - [(B-\varUpsilon)/2]^2 \tag{81}$$

As a result, (78) can also be expressed as:

$$q + \textstyle\sum_{n=1}^{2} \beta_n \le [(B+\varUpsilon)/2]^2 - [(B-\varUpsilon)/2]^2 \tag{82}$$

Now, (82) can be linearized using a piecewise-based linearization method:

$$q + \textstyle\sum_{n=1}^{2} \beta_n \le \sum_{\lambda=1}^{\varLambda} (m_\lambda^+ \delta_\lambda^+ + n_\lambda^+ \Delta_\lambda^+) - \sum_{\lambda=1}^{\varLambda} (m_\lambda^- \delta_\lambda^- + n_\lambda^- \Delta_\lambda^-) \tag{83}$$

$$(B+\varUpsilon)/2 = \textstyle\sum_{\lambda=1}^{\varLambda} \delta_\lambda^+ \quad , \quad (B-\varUpsilon)/2 = \sum_{\lambda=1}^{\varLambda} \delta_\lambda^- \tag{84}$$

$$\psi_{\lambda-1}^+ \Delta_\lambda^+ \le \delta_\lambda^+ \le \psi_\lambda^+ \Delta_\lambda^+ \quad , \quad \psi_{\lambda-1}^- \Delta_\lambda^- \le \delta_\lambda^- \le \psi_\lambda^- \Delta_\lambda^- \tag{85}$$

$$\textstyle\sum_{\lambda=1}^{\varLambda} \Delta_\lambda^+ \le 1 \quad , \quad \sum_{\lambda=1}^{\varLambda} \Delta_\lambda^- \le 1 \tag{86}$$

where the superscripts "+" and "−" respectively indicate the elements associated with the quadratic terms $[(B+\varUpsilon)/2]^2$ and $[(B-\varUpsilon)/2]^2$; $\delta_\lambda \ge 0$ and $\Delta_\lambda \in \{0,1\}$ respectively denote the continuous and binary auxiliary variables needed to obtain the piecewise linear expressions of quadratic terms; and ψ_λ, m_λ, and n_λ are constant parameters that can be obtained as follows:

$$\psi_\lambda^+ = (\lambda)(1/\varLambda)\overline{[(B+\varUpsilon)/2]} \quad , \quad \psi_\lambda^- = (\lambda)(1/\varLambda)\overline{[(B-\varUpsilon)/2]} \tag{87}$$

$$m_\lambda^+ = [(\psi_\lambda^+)^2 - (\psi_{\lambda-1}^+)^2]/[\psi_\lambda^+ - \psi_{\lambda-1}^+] \tag{88}$$

$$m_\lambda^- = [(\psi_\lambda^-)^2 - (\psi_{\lambda-1}^-)^2]/[\psi_\lambda^- - \psi_{\lambda-1}^-] \tag{89}$$

$$n_\lambda^+ = (\psi_\lambda^+)^2 - m_\lambda^+ \psi_\lambda^+ \quad , \quad n_\lambda^- = (\psi_\lambda^-)^2 - m_\lambda^- \psi_\lambda^- \tag{90}$$

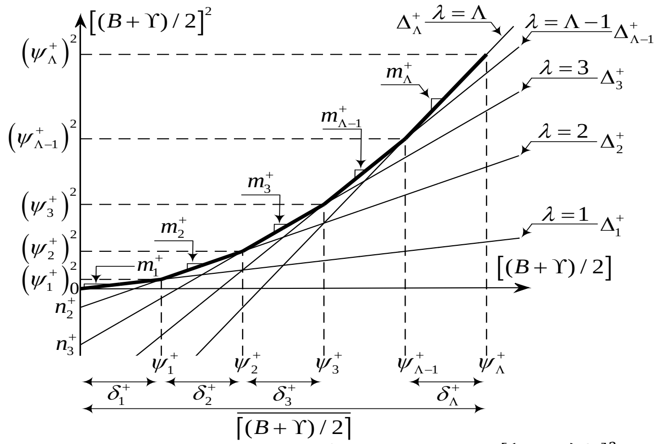

Fig. 1. Piecewise linear approximation of the quadratic term $[(B+\Upsilon)/2]^2$.

To clarify the proposed linearization method, the piecewise linear approximation of the quadratic term $[(B+\Upsilon)/2]^2$ is illustrated in Fig. 1. As can be seen, the distance between zero and $\lceil (B+\Upsilon)/2 \rceil$ is first partitioned into Λ segments. Then, corresponding to each segment λ, a line with the slope of m_λ and intercept of n_λ is considered. Finally, using the binary variables denoted by Δ_λ, only one of the lines is chosen to represent the quadratic term $[(B+\Upsilon)/2]^2$.

2) Linearization of Constraints (79) and (80)

With the help of some auxiliary variables (p_n, h_n, d_n), (79) and (80) can be simplified and rewritten as:

$$p_n = p_n^L - p_n^U \qquad \forall n = 1,2 \tag{91}$$

$$h_n = h_n^L - h_n^U \qquad \forall n = 1,2 \tag{92}$$

$$d_n = p_n + \Upsilon A_n \qquad \forall n = 1,2 \tag{93}$$

$$(p_n)^2 \leq -4\alpha_n h_n \qquad \forall n = 1,2 \tag{94}$$

$$(d_n)^2 \leq -4\beta_n h_n \qquad \forall n = 1,2 \tag{95}$$

Now, (93) can be linearized in a similar way as (78) by employing the above-described piecewise-based linearization method. On the other hand, the right-hand sides of (94) and (95) can be expressed as follows:

$$-4\alpha_n h_n = (\alpha_n - h_n)^2 - (\alpha_n + h_n)^2 \tag{96}$$

$$-4\beta_n h_n = (\beta_n - h_n)^2 - (\beta_n + h_n)^2 \tag{97}$$

Therefore, (94) and (95) can be written as:

$$\alpha_n - h_n \geq \sqrt{(p_n)^2 + (\alpha_n + h_n)^2} \qquad \forall n = 1,2 \tag{98}$$

$$\beta_n - h_n \geq \sqrt{(d_n)^2 + (\beta_n + h_n)^2} \qquad \forall n = 1,2 \tag{99}$$

Obviously, (98) and (99) are second-order conic constraints that have the same form as (57). Hence, they can be linearized using the polyhedral-based method described in Section III-C.

V. Simulation Results and Discussion

In this section, the most important results obtained from the implementation of the proposed planning methodology are presented and discussed. All the simulations have been implemented on a PC with a 3.40 GHz Intel Core i7-4770 processor and 16 GB of RAM using CPLEX 12.6.1 [42].

A. Test System Description

A 24-node distribution system, based on [11], is utilized to carry out the simulations. This test system consists of 4 substations, 20 load nodes, and 33 feeder sections. The set of candidate nodes for DG installation is defined as $\Omega^{NG} = \{1,2,3,4,5,7,9,13,15,16,17,18,19\}$. As an illustrative example, the renewable DGs are here assumed to be wind turbines, but the proposed methodology is fully applicable to other renewable DG technologies such as photovoltaic panels. The one-line diagram of the system as well as detailed data related to the power demands, candidate conductor types, alternatives for construction and reinforcement of substations, alternatives for installation of renewable/conventional DGs, lengths of feeder sections, and other parameters of the problem can be downloaded from [43].

B. A Discussion on the Accuracy and Computation Time of the Proposed Deterministic MILP Model

By ignoring the uncertainties, a comparative analysis is conducted here to assess the performance of the deterministic MILP model proposed in Section III-C from the aspects of accuracy and computational efficiency. The logic behind this comparative analysis is illustrated in Fig. 2. As can be seen, the MISOCP model developed in Section III-B is exact and does not involve any approximations. Based on this fact, we have used the MISOCP model as a benchmark against which the approximate MILP models can be compared. In this regard, first the MISOCP model is solved and the global optimal solution of the problem is found. This solution is then used as a benchmark for assessing the solution quality of two different approximate MILP models: 1) our proposed polyhedral-based MILP model; and 2) a piecewise-based MILP model presented in [16]. The main reason for choosing the model presented in [16] is that it is the most accurate MILP model existing in the literature.

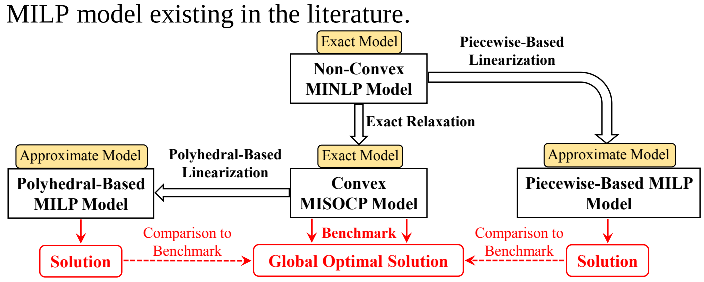

Fig. 2. Illustration of the logic behind the conducted comparative analysis.

The investment, operation, and total costs obtained by solving the MISOCP model are US\$6,699,691, US\$31,892,808, and US\$38,592,499, respectively. The MISOCP model, in spite of its ability to find the global optimal solution of the MDEP problem, is time-consuming and requires 182 min to be solved. This fact demonstrates the necessity of introducing an MILP model that is able to significantly improve the computational efficiency. Table I compares our proposed polyhedral-based MILP model with the piecewise-based MILP model presented in [16] from the accuracy and computation time perspectives. Note that the errors presented in this table indicate the amount by which the solutions of the MILP models deviate from the global optimal solution found by the MISOCP model. These errors are calculated as follows:

$$Error = \frac{c^{MILP} - c^{MISOCP}}{c^{MISOCP}} \times 100\% \tag{100}$$

where c^{MILP} denotes the costs associated with the MILP models; c^{MISOCP} denotes the costs associated with the MISOCP model; and $Error$ is the percent error.

As can be seen, the accuracy of the piecewise-based model cannot be improved beyond a certain level, even if the linearization parameter is set to a large value such as 60 and 70. However, the polyhedral-based model is capable of reaching extremely high degrees of accuracy, so that setting the linearization parameter to 8 results in the accuracies of 100%, 99.99%, and 99.99% for the investment, operation, and total costs, respectively. On the other hand, by investigating the results shown in Table I, it can be realized that after spending almost the same amount of computation time on both models, the polyhedral-based model provides better solutions. For instance, as shown in the bold rows of the table, when a computation time of 15 min is spent on the polyhedral-based model, the errors in the investment, operation, and total costs are notably lower than the case in which 17 min is spent on the piecewise-based model. These facts prove the superiority of the polyhedral-based model over the piecewise-based model. Moreover, our proposed MILP model is obviously able to provide the same solution as the MISOCP model, while its required computation time is around 12 times shorter than that of the MISOCP model. Given these results, it can concluded that the MILP model developed in section III-C has a great performance in deterministic planning studies of ADNs.

TABLE I
COMPARING THE PERFORMANCES OF THE POLYHEDRAL-BASED AND PIECEWISE-BASED DETERMINISTIC MILP MODELS

Deterministic MILP model	Linearization parameter	Errors in different costs (%)			Time (min)
		Inv.	Oper.	Total	
Polyhedral-based	3	+ 2.91	+ 1.47	+ 0.71	4.5
	4	+ 1.83	+ 0.98	+ 0.49	5
	5	+ 0.35	+ 0.62	+ 0.45	8
	6	+ 0.00	+ 0.34	+ 0.28	9.5
	7	+ 0.00	+ 0.05	+ 0.04	12
	8	+ **0.00**	+ **0.01**	+ **0.01**	**15**
Piecewise-based	10	+ 3.62	+ 2.34	+ 2.56	3
	20	+ 2.54	+ 1.24	+ 1.47	4
	30	+ 1.97	+ 0.93	+ 1.11	6.5
	40	+ 1.97	+ 1.08	+ 1.23	10
	50	+ 1.97	+ 1.26	+ 1.38	13
	60	+ 1.97	+ 0.99	+ 1.16	14.5
	70	+ **1.97**	+ **1.15**	+ **1.29**	**17**

Note that in the above discussion, the accuracy evaluation of the MILP models was conducted based the errors in the investment, operation, and total costs. These errors are the most reliable indices that can be used to evaluate the accuracy of the MILP models because any inaccuracy in these models will cause their investment, operation, and total costs to deviate from the global optimal values found by the MISOCP model. Nevertheless, other types of accuracy evaluation indices may also be utilized. In [16], for instance, the error in the active power loss is used as an index for evaluating the accuracy of the proposed MILP model.

C. Robustness Evaluation of the Proposed DRCC-MILP Model

In this subsection, we demonstrate the robustness of the proposed DRCC-MILP model against the uncertain wind generations and loads having various types of PDFs. This model is also compared with two other models based on the deterministic and Gaussian chance-constrained (GCC) approaches that are widely used in the existing literature [7-11], [16], [26-28]. That is, the following three models are considered:

- **Model 1:** Deterministic MILP model in which, similar to [7-11], [16], the uncertainties are totally ignored.
- **Model 2:** GCC-MILP model in which, similar to [26-28], all the uncertainties are assumed to be Gaussian distributed.
- **Model 3:** Proposed DRCC-MILP model in which the uncertainty distributions are assumed to be unknown.

In order to build the ambiguity set ($\mathcal{D}$) required by Model 3, the confidence intervals of the first and second moments of the random variables need to be specified. These confidence intervals should be defined based on historical data of random variables. In this regard, given a series of data samples $\{\tilde{\chi}_{n,w}\}_{w=1}^{\mathcal{W}}$ for the random variable $\tilde{\chi}_n$, the estimated values of the first and second moments can be obtained using the following formulas:

$$\widehat{\mu_n} = \frac{1}{\mathcal{W}} \sum_{w=1}^{\mathcal{W}} \tilde{\chi}_{n,w} \qquad \forall n = 1,2 \qquad (101)$$

$$\widehat{\sigma_n} = \frac{1}{\mathcal{W}} \sum_{w=1}^{\mathcal{W}} \left(\tilde{\chi}_{n,w} - \widehat{\mu_n}\right)^2 \qquad \forall n = 1,2 \qquad (102)$$

where $\widehat{\mu_n}$ denotes the estimated value of the first moment of the nth random variable; $\widehat{\sigma_n}$ denotes the estimated value of the second moment of the nth random variable; $\tilde{\chi}_{n,w}$ denotes the wth data sample of the nth random variable; and $\mathcal{W}$ is the total number of data samples. Now, the confidence intervals $[\underline{\mu_n}, \overline{\mu_n}]$ and $[\underline{\sigma_n}, \overline{\sigma_n}]$ can be obtained by defining reasonable ranges around $\widehat{\mu_n}$ and $\widehat{\sigma_n}$, respectively. Defining a wider range around $\widehat{\mu_n}$ or $\widehat{\sigma_n}$ will obviously result in robustness against a larger family of PDFs. In this paper, the historical wind generation and load data are acquired from [44], [45], respectively. These historical data are converted to per-unit values and utilized to calculate $\widehat{\mu_n}$ and $\widehat{\sigma_n}$. The obtained values are as follows: $\widehat{\mu_1}$ = 0.427, $\widehat{\mu_2}$ = 0.988, $\widehat{\sigma_1}$ = 0.0519, and $\widehat{\sigma_2}$=0.0126. Considering plausible ranges around these values, the confidence intervals are defined as $[\underline{\mu_1}, \overline{\mu_1}]$ = [0.3, 0.5], $[\underline{\mu_2}, \overline{\mu_2}]$ = [0.95, 1.05], $[\underline{\sigma_1}, \overline{\sigma_1}]$ = [0.02, 0.08], and $[\underline{\sigma_2}, \overline{\sigma_2}]$ = [0.01, 0.02]. Note that these confidence intervals can be flexibly tailored to meet the decision maker's requirements.

After solving Models 1-3, their solution robustness is assessed considering several different PDFs for wind generation and load. To this end, as shown in Fig. 3, three typical PDFs are considered for each of the random variables $\widetilde{\chi^{GR}}$and $\widetilde{\chi^{D}}$. Then, regarding all combinations of W1-W3 and L1-L3, a total number of nine test cases are defined for PDFs of wind generation and load. Lastly, under each defined PDF case, 10000 samples of wind generation and load are produced and used for robustness evaluations.

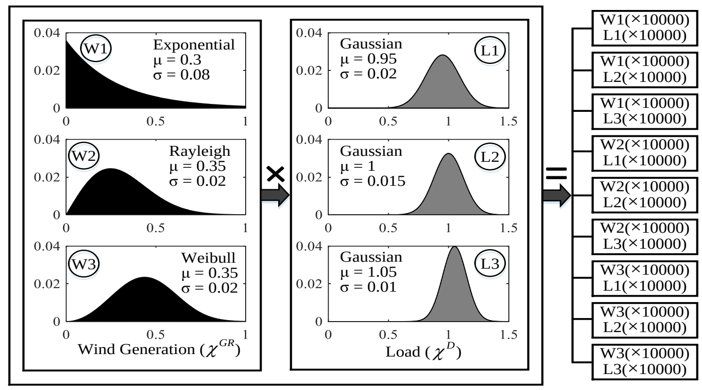

Fig. 3. Illustration of the nine test cases defined for PDFs of wind generation and load (μ and σ denote the first and second moments, respectively).

Table II compares the performances of Models 1-3 from the viewpoints of solution robustness, investment cost, and computation time, while considering two different risk parameters (ϵ = 0.1 and ϵ = 0.05). In this table, the abbreviations Avg., Min., and Max. respectively represent the average, minimum, and maximum of the robustness levels found by testing the defined PDF cases. The details of the robustness levels of Models 1-3 for each PDF case are also provided in Fig. 4. As can be observed, Model 1 has the lowest level of robustness, with an average of only 29.86%. This poor performance is obviously due to the fact that Model 1 does not have any information about the uncertainties when deciding about the expansion plans. Model 2 results in higher robustness levels; however, as can be seen in Fig. 4, its robustness is always below the requirement (i.e., $1-\epsilon$) for different PDF cases. The reason is that Model 2 finds the solution of the MDEP problem assuming Gaussian PDFs for wind generation and load and, hence, it cannot sufficiently account for other types of uncertainty distributions. In contrast, Model 3 is highly robust against the uncertainties and, as illustrated in Fig. 4, its robustness is considerably higher than the specified level (i.e., $1-\epsilon$) under all PDF cases. Moreover, taking a careful look at Fig. 4 reveals that when $1-\epsilon$ = 90%, the robustness of Model 2 is significantly lower than when $1-\epsilon$ = 95%. In contrast, the robustness of Model 3 is very high for both ϵ=0.1 and ϵ=0.05, which implies that this model is less sensitive to the risk parameter ϵ. It should be noted that, as expected, the higher robustness of Model 3 is obtained at the cost of a small increase in computation time and investment. Nevertheless, it is worth to bear such a reasonable cost to achieve the reported substantial improvement in the robustness of the solution. To sum up, it can be stated that Model 3 makes an appropriate trade-off among the solution robustness, investment cost, and computational burden as compared to the other two models.

TABLE II
PERFORMANCE COMPARISON OF MODELS 1-3 FROM THE VIEWPOINTS OF SOLUTION ROBUSTNESS, INVESTMENT COST, AND COMPUTATION TIME

MDEP Models		Model 1	Model 2		Model 3	
$1-\epsilon$ (%)		N/A	90	95	90	95
Robustness (%)	Avg.	29.86	41.94	77.26	96.81	98.80
	Min.	10.54	18.99	59.74	94.82	97.94
	Max.	49.18	68.27	90.43	97.76	99.61
Investment (10^6 US$)		6.699	6.851	6.946	7.083	7.157
Time (min)		15	22	24	29.5	33

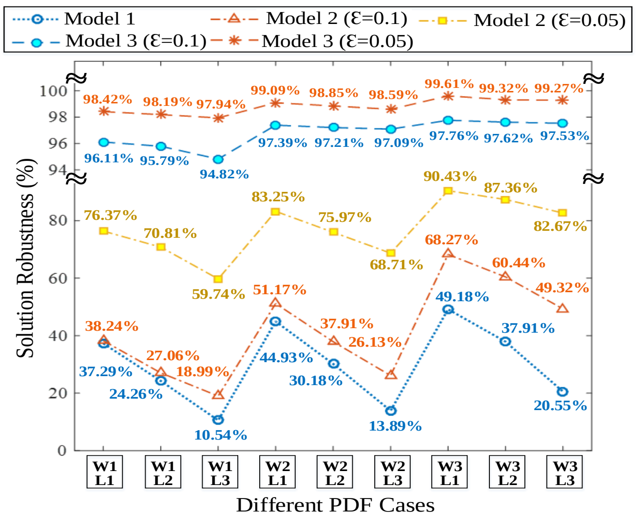

Fig. 4. Solution robustness of Models 1-3 for different PDF cases.

D. *Sensitivity Analysis of Robustness of the DRCC-MILP Model*

As described in Section IV-C, a combination of two linearization methods was utilized to overcome the nonlinearities of the DR reformulation of CCs: polyhedral approximation and piecewise approximation. In this subsection, we analyze the impacts of the accuracy of these linearization methods on the robustness of the proposed DRCC-MILP model.

The accuracy of the polyhedral approximation depends on a parameter denoted by $\mathcal{L}$, so that the approximation error decreases as $\mathcal{L}$ is increased. In Section III-C, it was shown that choosing an appropriate value for $\mathcal{L}$ causes the polyhedral approximation to be highly accurate. For instance, based on (62), setting $\mathcal{L}$ to 8 results in an approximation error of ϱ=1.88 × 10^{-5}, which is equivalent to an accuracy of almost 100%. Based on this fact, it can be stated that when $\mathcal{L}$ is greater than or equal to 8, the high accuracy of the polyhedral approximation is ensured. Thus, in order to linearize the DR reformulation of CCs, we have chosen $\mathcal{L}$=8 to make sure about the high accuracy of the polyhedral approximation.

On the other hand, the accuracy of the piecewise approximation is dependent on a parameter denoted by Λ, which determines the number of segments used for linearization. By increasing Λ, the approximation error will obviously decrease. However, quantifying the effect of Λ on the accuracy of the piecewise approximation is not straightforward. As a result, we have conducted a sensitivity analysis to study the impacts of Λ on the robustness of the DRCC-MILP model. In this regard, Λ is changed from 5 to 20 in steps of 1, and the corresponding changes in the robustness of the DRCC-MILP model are examined. The obtained results are illustrated in Fig. 5. Note that the sensitivity analyses are performed for all the PDF cases defined in Section V-C while considering $\mathcal{L}$=8 and ϵ=0.1.

As can be seen, by increasing Λ in the range of 5 to 13, the robustness of the DRCC-MILP model is significantly improved. The reason is that in this range, an increase in Λ leads to a big improvement in the accuracy of the piecewise approximation, which causes the accuracy of the linearized DR reformulation of CCs to be considerably improved. However, increasing Λ in the range beyond 14 does not make a tangible improvement in the robustness of the DRCC-MILP model. This is because when Λ reaches a value of 14, the piecewise approximation achieves its highest accuracy level (almost 100%), and hence the solution robustness remains constant beyond Λ=14.

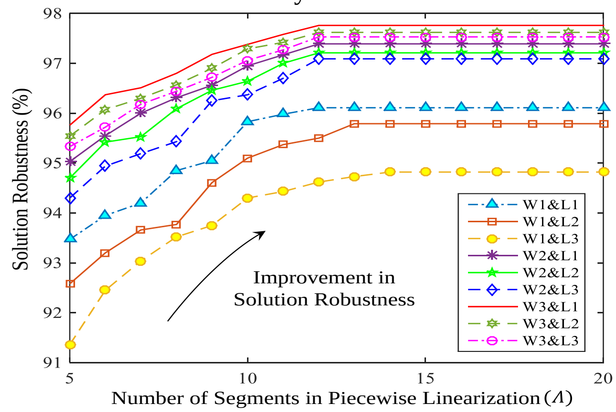

Fig. 5. Impact of the accuracy of the piecewise approximation on the robustness of the DRCC-MILP model.

Based on the above discussion, it can be stated that choosing suitable values for $\mathcal{L}$ and Λ causes the linearized DR reformulation of CCs to be highly accurate, so that the approximation errors have a negligible impact on the robustness of the DRCC-MILP model.

E. *Demonstration of the Scalability of the Proposed MILP Models*

A 138-node test system, based on [11], is here employed to demonstrate the scalability of the proposed MILP models (both deterministic and DRCC). This test system consists of 135 load nodes, 151 feeder sections, and 3 substations. The set of candidate nodes for DG installation is defined as Ω^{NG}={4,10,19,25,28,31, 42,52,56,64,68,72,78,85,94,97,100,103,106,108,111,116,120, 122,126,133}. The one-line diagram of the system and detailed data related to the power demands, candidate conductor types, lengths of feeder sections, alternatives for construction and reinforcement of substations, alternatives for installation of renewable/conventional DGs, and other parameters of the problem can be downloaded from [46].

The simulation results show that, for the linearization parameter of $\mathcal{L}$=8, the deterministic MILP model requires a computation time of 83 min to be solved. On the other hand, considering the risk parameter of ϵ=0.1 and the linearization parameters of $\mathcal{L}$=8 and Λ=14, the DRCC-MILP model consumes a computation time of 152 min to obtain the optimal solution of the MDEP problem. As can be seen, the proposed MILP models find the optimal expansion plans of the 138-node test system within reasonable computation times. This demonstrates another outstanding merit of the proposed MILP models, i.e., their ability to deal with the MDEP problem of large distribution systems in a computationally efficient manner.

One of the main purposes of our proposed planning methodology is to determine the optimal location, size, and type of DGs. This aspect is studied using the 138-node test system as it is large enough to provide a wide range of options for DG installation. In this regard, to investigate the impacts of the proposed DRCC programming approach on the DG deployment plans, we have compared the deterministic MILP model with the DRCC-MILP model from the viewpoints of the location, size, and type of the installed DGs, as shown in Table III. In this table, "C" and "R" stand for "conventional" and "renewable", respectively.

As can be seen, three DG locations (i.e., 10, 28, and 108) are the same for both models. However, the sizes and types of DGs are different for the deterministic and DRCC models. When utilizing the deterministic model, the uncertainties of renewable generations are entirely ignored. This causes the deterministic model to deploy more renewable DGs (7 MW) than conventional ones (4 MW) because renewable DGs do not have any generation costs. However, when the DRCC model is used, the uncertainties of renewable DGs are incorporated into the optimization process. As a result, the DRCC model deploys less renewable DGs (3 MW) to obtain more robust expansion plans. This fact implies that the robustness of the expansion plans has an inverse relationship with the penetration of renewable DGs. Hence, making a proper trade-off between these two conflicting factors is of great importance.

TABLE III
COMPARISON OF THE DETERMINISTIC MILP AND DRCC-MILP MODELS FROM THE VIEWPOINT OF DG DEPLOYMENT

MDEP Models	Specifications of the installed DGs							
Deterministic MILP	Location	10	28	72	85	100	108	133
	Size (MW)	1	2	2	1	1	2	2
	Type	C	R	R	C	R	R	C
DRCC-MILP	Location	10	28	56	94	97	111	108
	Size (MW)	2	1	2	1	1	1	1
	Type	C	R	C	C	R	C	R

VI. CONCLUSION

In this paper, a novel DRCC-MILP model has been proposed for the MDEP problem of ADNs, which has three notable merits: first, it incorporates a highly accurate linearized network model reflecting AC power flow equations and energy losses; second, it immunizes the expansion plans against the uncertain renewable generations and loads with unknown PDFs; and third, its linear formulation ensures computational tractability and solution optimality. The proposed planning methodology has been successfully validated using two different distribution systems. The simulation results show that, with regard to network modelling, the MILP model developed in this paper offers a higher degree of accuracy than the most accurate MILP model existing in the literature, while both models consume almost the same amount of computation time. Furthermore, after testing the uncertain renewable generations and loads with several different PDFs, the results demonstrate the significantly higher robustness of the proposed DRCC-MILP model compared to the deterministic and Gaussian chance-constrained MILP models.

REFERENCES

[1] M. Sedghi, A. Ahmadian, and M. Aliakbar-Golkar, "Optimal storage planning in active distribution network considering uncertainty of wind power distributed generation," *IEEE Trans. Power Syst.*, vol. 31, pp. 304-316, 2016.

[2] V. F. Martins and C. L. Borges, "Active distribution network integrated planning incorporating distributed generation and load response uncertainties," *IEEE Trans. Power Syst.*, vol. 26, pp. 2164-2172, 2011.

[3] M. Asensio, P. M. de Quevedo, G. Munoz-Delgado, and J. Contreras, "Joint distribution network and renewable energy expansion planning considering demand response and energy storage - part I: stochastic programming model," *IEEE Trans. Smart Grid*, 2016 (Early Access).

[4] M. Asensio, P. M. de Quevedo, G. Munoz-Delgado, and J. Contreras, "Joint distribution network and renewable energy expansion planning considering demand response and energy storage - part II: numerical results and considered metrics," *IEEE Trans. Smart Grid*, 2016 (Early Access).

[5] P. S. Georgilakis and N. D. Hatziargyriou, "A review of power distribution planning in the modern power systems era: Models, methods and future research," *Electr. Power Syst. Res.*, vol. 121, pp. 89-100, 2015.

[6] W. Yao, C. Y. Chung, F. Wen, M. Qin, and Y. Xue, "Scenario-based comprehensive expansion planning for distribution systems considering integration of plug-in electric vehicles," *IEEE Trans. Power Syst.*, vol. 31, pp. 317-328, 2016.

[7] J. Aghaei, K. M. Muttaqi, A. Azizivahed, and M. Gitizadeh, "Distribution expansion planning considering reliability and security of energy using modified PSO (Particle Swarm Optimization) algorithm," *Energy*, vol. 65, pp. 398-411, 2014.

[8] K. M. Muttaqi, A. D. Le, J. Aghaei, E. Mahboubi-Moghaddam, M. Negnevitsky, and G. Ledwich, "Optimizing distributed generation parameters through economic feasibility assessment," *Applied Energy*, vol. 165, pp. 893-903, 2016.

[9] M. Nayeripour, E. Mahboubi-Moghaddam, J. Aghaei, and A. Azizi-Vahed, "Multi-objective placement and sizing of DGs in distribution networks ensuring transient stability using hybrid evolutionary algorithm," *Renewable and Sustainable Energy Reviews*, vol. 25, pp. 759-767, 2013.

[10] S. Haffner, L. F. A. Pereira, L. A. Pereira, and L. S. Barreto, "Multistage model for distribution expansion planning with distributed generation - part I: problem formulation," *IEEE Trans. Power Del.*, vol. 23, pp. 915-923, 2008.

[11] G. Muñoz-Delgado, J. Contreras, and J. M. Arroyo, "Joint expansion planning of distributed generation and distribution networks," *IEEE Trans. Power Syst.*, vol. 30, pp. 2579-2590, 2015.

[12] G. Muñoz-Delgado, J. Contreras, and J. M. Arroyo, "Multistage generation and network expansion planning in distribution systems considering uncertainty and reliability," *IEEE Trans. Power Syst.*, vol. 31, pp. 3715-3728, 2016.

[13] S. F. Santos, D. Z. Fitiwi, A. W. Bizuayehu, M. Shafie-khah, M. Asensio, J. Contreras, *et al.*, "Novel multi-stage stochastic DG investment planning with recourse," *IEEE Trans. Sustain. Energy* vol. 8, pp. 164-178, 2017.

[14] M. Asensio, G. Munoz-Delgado, and J. Contreras, "A bi-level approach to distribution network and renewable energy expansion planning considering demand response," *IEEE Trans. Power Syst.*, 2017 (Early Access).

[15] S. F. Santos, D. Z. Fitiwi, M. Shafie-Khah, A. W. Bizuayehu, C. M. Cabrita, and J. P. Catalão, "New multistage and stochastic mathematical model for maximizing RES hosting capacity - part I: problem formulation," *IEEE Trans. Sustain. Energy*, vol. 8, pp. 304-319, 2017.

[16] A. Tabares, J. F. Franco, M. Lavorato, and M. J. Rider, "Multistage long-term expansion planning of electrical distribution systems considering multiple alternatives," *IEEE Trans. Power Syst.*, vol. 31, pp. 1900-1914, 2016.

[17] J. Zhan, C. Y. Chung, and A. Zare, "A fast solution method for stochastic transmission expansion planning," *IEEE Trans. Power Syst.*, 2017 (Early Access).

[18] S. N. Ravadanegh, N. Jahanyari, A. Amini, and N. Taghizadeghan, "Smart distribution grid multistage expansion planning under load forecasting uncertainty," *IET Gener. Transm. Distrib.* , vol. 10, pp. 1136-1144, 2016.

[19] M. Dadkhah and B. Venkatesh, "Cumulant based stochastic reactive power planning method for distribution systems with wind generators," *IEEE Trans. Power Syst.*, vol. 27, pp. 2351-2359, 2012.

[20] A. Kavousi-Fard, T. Niknam, and M. Fotuhi-Firuzabad, "Stochastic reconfiguration and optimal coordination of V2G plug-in electric vehicles considering correlated wind power generation," *IEEE Trans. Sustain. Energy*, vol. 6, pp. 822-830, 2015.

[21] Z. Wang, B. Chen, J. Wang, J. Kim, and M. M. Begovic, "Robust optimization based optimal DG placement in microgrids," *IEEE Trans. Smart Grid*, vol. 5, pp. 2173-2182, 2014.

[22] P. Xiong, P. Jirutitijaroen, and C. Singh, "A distributionally robust optimization model for unit commitment considering uncertain wind power generation," *IEEE Trans. Power Syst.*, vol. 32, pp. 39-49, 2017 (Early Access).

[23] C. Zhao and R. Jiang, "Distributionally robust contingency-constrained unit commitment," *IEEE Trans. Power Syst.*, 2017 (Early Access).

[24] A. Ben-Tal and A. Nemirovski, "On polyhedral approximations of the second-order cone," *Mathematics of Operations Research*, vol. 26, pp. 193-205, 2001.

[25] A. Charnes and W. W. Cooper, "Chance-constrained programming," *Management science*, vol. 6, pp. 73-79, 1959.

[26] J. F. Franco, M. J. Rider, and R. Romero, "Robust multi-stage substation expansion planning considering stochastic demand," *IEEE Trans. Power Syst.*, vol. 31, pp. 2125-2134, 2016.

[27] D. Bienstock, M. Chertkov, and S. Harnett, "Chance-constrained optimal power flow: Risk-aware network control under uncertainty," *SIAM Review*, vol. 56, pp. 461-495, 2014.

[28] D. Bienstock, M. Chertkov, and S. Harnett, "Robust modeling of probabilistic uncertainty in smart grids: data ambiguous chance constrained optimum power flow," in *Decision and Control (CDC), 2013 IEEE 52nd Annual Conference on*, 2013, pp. 4335-4340.

[29] F. Qiu and J. Wang, "Distributionally robust congestion management with dynamic line ratings," *IEEE Trans. Power Syst.*, vol. 30, pp. 2198-2199, 2015.

[30] F. Qiu and J. Wang, "Chance-constrained transmission switching with guaranteed wind power utilization," *IEEE Trans. Power Syst.*, vol. 30, pp. 1270-1278, 2015.

[31] R. Jiang and Y. Guan, "Data-driven chance constrained stochastic program," *Mathematical Programming*, vol. 158, pp. 291-327, 2016.

[32] A. Shapiro, "On duality theory of conic linear problems," in *Semi-infinite programming*, ed: Springer, 2001, pp. 135-165.

[33] V. A. Yakubovich, "S-procedure in nonlinear control theory," *Vestnik Leningrad University*, vol. 1, pp. 62-77, 1971.

[34] M. E. Baran and F. F. Wu, "Optimal capacitor placement on radial distribution systems," *IEEE Trans. Power Del.*, vol. 4, pp. 725-734, 1989.

[35] R. Cespedes, "New method for the analysis of distribution networks," *IEEE Trans. Power Del.*, vol. 5, pp. 391-396, 1990.

[36] J. F. Franco, M. J. Rider, M. Lavorato, and R. Romero, "Optimal conductor size selection and reconductoring in radial distribution systems using a mixed-integer LP approach," *IEEE Trans. Power Syst.*, vol. 28, pp. 10-20, 2013.

[37] M. Lavorato, J. F. Franco, M. J. Rider, and R. Romero, "Imposing radiality constraints in distribution system optimization problems," *IEEE Trans. Power Syst.*, vol. 27, pp. 172-180, 2012.

[38] M. Farivar and S. H. Low, "Branch flow model: relaxations and convexification-part I," *IEEE Trans. Power Syst.*, vol. 28, pp. 2554-2564, 2013.

[39] L. Roald and G. Andersson, "Chance-Constrained AC Optimal Power Flow: Reformulations and Efficient Algorithms," *IEEE Trans. Power Syst.*, 2017 (Early Access).

[40] X. Chen and Y. Zhang, "Uncertain linear programs: extended affinely adjustable robust counterparts," *Operations Research*, vol. 57, pp. 1469-1482, 2009.

[41] A. Ben-Tal, A. Goryashko, E. Guslitzer, and A. Nemirovski, "Adjustable robust solutions of uncertain linear programs," *Mathematical Programming*, vol. 99, pp. 351-376, 2004.

[42] IBM ILOG CPLEX Optimization Studio, [Online]. Available: www-03.ibm.com/software/products/en/ibmilogcpleoptistud

[43] Data Related to the 24-Node Test System, [Online]. Available: www.dropbox.com/s/q4sde5400fa35pp/24node%20test%20system%20data.pdf?dl=0

[44] Hourly Historical Data of Wind Generation, [Online]. Available: www.pjm.com/markets-and-operations/ops-analysis.aspx

[45] Hourly Historical Data of Load, [Online]. Available: www.pjm.com/markets-and-operations/ops-analysis/historical-load-data.aspx

[46] Data Related to the 138-Node Test System, [Online]. Available: www.dropbox.com/s/2w4mg322wtw8qun/138node%20test%20system%20data.pdf?dl=0

Alireza Zare (S'14) received the B.Sc. degree in electrical engineering from Shahid Rajaee Teacher Training University, Tehran, Iran, in 2012, and the M.Sc. degree in electrical engineering from Sharif University of Technology, Tehran, Iran, in 2014. In September 2015, he joined the Department of Electrical and Computer Engineering at the University of Saskatchewan, Canada, where he is currently working toward the Ph.D. degree in electrical engineering.

His research interests include distribution system planning and operation, renewable and distributed energy resources, microgrid planning and operation, energy management of electric vehicles, and smart grid technologies.

C. Y. Chung (M'01–SM'07–F'16) received the B.Eng. (with First Class Honors) and Ph.D. degrees in electrical engineering from The Hong Kong Polytechnic University, Hong Kong, China, in 1995 and 1999, respectively.

He has worked for Powertech Labs, Inc., Surrey, BC, Canada; the University of Alberta, Edmonton, AB, Canada; and The Hong Kong Polytechnic University, China. He is currently a Professor, the NSERC/SaskPower (Senior) Industrial Research Chair in Smart Grid Technologies, and the SaskPower Chair in Power Systems Engineering in the Department of Electrical and Computer Engineering at the University of Saskatchewan, Saskatoon, SK, Canada. His research interests include smart grid technologies, renewable energy, power system stability/control, planning and operation, computational intelligence applications, power markets and electric vehicle charging.

Dr. Chung is an Editor of IEEE Transactions on Power Systems and IEEE Transactions on Sustainable Energy. He is also an IEEE PES Distinguished Lecturer and a Member-at-Large (Global Outreach) of the IEEE PES Governing Board.

Junpeng Zhan (M'16) received the B.Eng. and Ph.D. degrees in electrical engineering from Zhejiang University, Hangzhou, China, in 2009 and 2014, respectively.

He is currently a Postdoctoral Fellow in the Department of Electrical and Computer Engineering, University of Saskatchewan, Saskatoon, SK, Canada. His current research interests include integration of the energy storage systems, dynamic thermal rating, and renewable electric energy sources in power systems.

Sherif Omar Faried (S'88–M'88–SM'00) received the B.Sc. and M.Sc. degrees from Ain Shams University, Cairo, Egypt, in 1979 and 1984, respectively, and the M.Sc. and Ph.D. degrees from the University of Saskatchewan, Saskatoon, SK, Canada, in 1988 and 1993, respectively, all in electrical engineering.

From 1979 to 1984, he was a Teaching and Research Assistant in the Department of Electrical Power and Machines, Ain Shams University. He is currently a Professor of Electrical Engineering in the Department of Electrical and Computer Engineering, University of Saskatchewan. His current research interests include power system dynamics, control, reliability, protection, and power quality.

Prof. Faried is a Registered Professional Engineer in the Province of Saskatchewan, Canada.